

Decays and spectrum of bottom and bottom strange mesons

Ishrat Asghar and Bilal Masud

Centre For High Energy Physics, Punjab University, Lahore(54590), Pakistan.

E. S. Swanson

University of Pittsburgh, Pittsburgh PA 15260, USA.

Faisal Akram and M. Atif Sultan

Centre For High Energy Physics, Punjab University, Lahore(54590), Pakistan.

Abstract

The strong decay amplitudes and radiative partial widths of orbital and radially excited states of B and B_s mesons are presented. These results are obtained with a nonrelativistic potential quark model, the nonrelativistic reduction of the electromagnetic transition operator, and the “ 3P_0 ” model of strong decays. The predictions are compared to experiment where possible and assignments for the recently discovered states, $B_1(5721)$, $B_2^*(5747)$, $B_J(5840)$, $B_J(5970)$, $B_{s1}(5830)$, and $B_{s2}^*(5840)$, are made.

I. INTRODUCTION

In 2007 the DO collaborations[1] announced the discoveries of bottom mesons $B_1(5721)$ and $B_2^*(5747)$. This was followed with sightings of the $B_{s1}(5830)$ and $B_{s2}^*(5840)$ states at LHCb[2] in 2013. More recently CDF[3] and LHCb[4] have found evidence for excited bottom mesons, $B_J(5970)$ and $B_J(5940)$. These recent discoveries of bottom and bottom-strange mesons motivate model computations in these sectors. The immediate goal is to assist in identifying these states, while a longer term goal is to determine the limits of potential models as useful descriptions of low lying hadrons. To this end we construct a reasonably “standard” nonrelativistic potential quark model and fit its parameters to the known B and B_s mesons. The philosophy underpinning this type of modelling is the adiabatic separation of “slow” constituent quark degrees of freedom from “fast” gluonic degrees of freedom [5–8]. The spectrum and wavefunctions that emerge from this computation are used to compute E1 and M1 radiative transitions. Finally, the “ 3P_0 ” model of strong decays, wherein it is assumed that quark-antiquark pairs are created with vacuum quantum numbers, is used to compute open flavour decays of a collection of low lying B and B_s states.

The organization of the paper is as follows. First, we describe the potential model used to calculate the mass spectrum of the bottom and bottom-strange mesons. Mixed states are discussed in Sec. II A along with conventions used in the literature. In Sec. III, we review the 3P_0 decay model evaluation of strong decay amplitudes using simple harmonic oscillator (SHO) wave functions. E1 and M1 radiative transitions are calculated in Sec. IV. The results of these computations are compared with available experimental data in Sec. V, while our conclusions are given in Sec. VI.

II. CONSTITUENT QUARK MODEL FOR B AND B_s STATES

The chief assumptions underpinning our model are nonrelativistic kinematics, a “Coulomb+linear” central potential, and spin-dependent corrections generated from vector gluon exchange and an effective scalar confinement interaction. While it is relatively simple to incorporate relativistic kinematics for the quarks, these effects can be largely subsumed into the constituent quark mass, and in fact, there is evidence that this is a preferred approach[9, 10].

The potential used in this paper is given by

$$V_{q\bar{q}}(r) = -\frac{4\alpha_s}{3r} + br + \frac{32\pi\alpha_s}{9m_q m_{\bar{q}}} \left(\frac{\sigma}{\sqrt{\pi}}\right)^3 e^{-\sigma^2 r^2} \mathbf{S}_q \cdot \mathbf{S}_{\bar{q}} + \frac{4\alpha_s}{m_q m_{\bar{q}} r^3} T \\ + \left(\frac{\mathbf{S}_q}{8m_q^2} + \frac{\mathbf{S}_{\bar{q}}}{8m_{\bar{q}}^2} \right) \cdot \mathbf{L} \left(\frac{4\alpha_s}{3r^3} - \frac{b}{r} \right) + \frac{\mathbf{S}_q + \mathbf{S}_{\bar{q}}}{4m_q m_{\bar{q}}} \cdot \mathbf{L} \frac{4\alpha_s}{3r^3}. \quad (1)$$

Here α_s is the strong coupling constant, b is the string tension, and T is the tensor operator

$$T = \mathbf{S}_q \cdot \hat{r} \mathbf{S}_{\bar{q}} \cdot \hat{r} - \frac{1}{3} \mathbf{S}_q \cdot \mathbf{S}_{\bar{q}} \quad (2)$$

with diagonal matrix elements given by

$$T = \begin{cases} -\frac{L}{6(2L+3)} & J = L + 1 \\ \frac{1}{6} & J = L \\ -\frac{(L+1)}{6(2L-1)} & J = L - 1. \end{cases} \quad (3)$$

The parameters used in this potential for B and B_s mesons are taken to be $\sigma = 0.84 \text{ GeV}$, $\alpha_s(B) = 0.775$, $\alpha_s(B_s) = 0.642$ and $b = 0.0945 \text{ GeV}^2$. These values were obtained by fitting the masses of eight experimentally known states of B and B_s mesons (these are listed in 4th and 7th columns of Table I). The light quark masses, $m_{u/d}$ and m_s , were obtained from fits to light mesons. Finally, the bottom quark mass of Ref. [11] was used. These masses are

$$m_u = m_d = 0.325 \text{ GeV}, \\ m_s = 0.422 \text{ GeV}, \\ m_b = 4.825 \text{ GeV}. \quad (4)$$

The radial Schrödinger equation was solved with the shooting method[6]; results for the B and B_s spectrum are reported in Table I.

TABLE I: Masses of ground and radially excited states of B and B_s mesons.

n	Meson	Our calculated Mass (GeV)	Expt. Mass [12] (GeV)	Meson	Our calculated Mass (GeV)	Expt. Mass [12] (GeV)
1S	$B(1^1S_0)$	5.2675	5.27926 ± 0.00017	$B_s(1^1S_0)$	5.37697	5.36677 ± 0.00024
	$B(1^3S_1)$	5.32949	5.3252 ± 0.0004	$B_s(1^3S_1)$	5.42194	$5.4154^{+0.0024}_{-0.0021}$
2S	$B(2^1S_0)$	5.87731	...	$B_s(2^1S_0)$	5.92868	...
	$B(2^3S_1)$	5.90536	...	$B_s(2^3S_1)$	5.94895	...
3S	$B(3^1S_0)$	6.28798	...	$B_s(3^1S_0)$	6.30477	...
	$B(3^3S_1)$	6.30821	...	$B_s(3^3S_1)$	6.31925	...
4S	$B(4^1S_0)$	6.63061	...	$B_s(4^1S_0)$	6.61943	...
	$B(4^3S_1)$	6.64701	...	$B_s(4^3S_1)$	6.63109	...
1P	$B(1^3P_0)$	5.70364	...	$B_s(1^3P_0)$	5.76968	...
	$B(1^3P_2)$	5.76895	5.743 ± 0.005	$B_s(1^3P_2)$	5.82153	5.83996 ± 0.0002
	$B(1 P_1)$	5.75512	5.7235 ± 0.002	$B_s(1 P_1)$	5.80299	5.8287 ± 0.0004
	$B(1 P'_1)$	5.73920	...	$B_s(1 P'_1)$	5.80095	...
	ϕ_{1P}	35.3°		ϕ_{1P}	35.3°	
2P	$B(2^3P_0)$	6.12867	...	$B_s(2^3P_0)$	6.15958	...
	$B(2^3P_2)$	6.18965	...	$B_s(2^3P_2)$	6.20834	...
	$B(2 P_1)$	6.17525	...	$B_s(2 P_1)$	6.19639	...
	$B(2 P'_1)$	6.1614	...	$B_s(2 P'_1)$	6.18615	...
	ϕ_{2P}	35.3°		ϕ_{2P}	35.3°	
3P	$B(3^3P_0)$	6.48027	...	$B_s(3^3P_0)$	6.48284	...
	$B(3^3P_2)$	6.53949	...	$B_s(3^3P_2)$	6.53036	...
	$B(3 P_1)$	6.52499	...	$B_s(3 P_1)$	6.51843	...
	$B(3 P'_1)$	6.51159	...	$B_s(3 P'_1)$	6.50828	...
	ϕ_{3P}	35.3°		ϕ_{3P}	35.3°	
1D	$B(1^3D_1)$	6.02239	...	$B_s(1^3D_1)$	6.05682	...
	$B(1^3D_3)$	6.03076	...	$B_s(1^3D_3)$	6.06293	...
	$B(1 D_2)$	6.03122	...	$B_s(1 D_2)$	6.06403	...
	$B(1 D'_2)$	6.02649	...	$B_s(1 D'_2)$	6.05935	...
	ϕ_{1D}	39.2°		ϕ_{1D}	39.2°	
2D	$B(2^3D_1)$	6.38438	...	$B_s(2^3D_1)$	6.39012	...
	$B(2^3D_3)$	6.39544	...	$B_s(2^3D_3)$	6.39853	...
	$B(2 D_2)$	6.39323	...	$B_s(2 D_2)$	6.39741	...
	$B(2 D'_2)$	6.39075	...	$B_s(2 D'_2)$	6.39453	...
	ϕ_{2D}	39.2°		ϕ_{2D}	39.2°	
1F	$B(1^3F_2)$	6.25908	...	$B_s(1^3F_2)$	6.27319	...
	$B(1^3F_4)$	6.252	...	$B_s(1^3F_4)$	6.26679	...
	$B(1 F_3)$	6.2637	...	$B_s(1 F_3)$	6.27694	...
	$B(1 F'_3)$	6.24939	...	$B_s(1 F'_3)$	6.26467	...
	ϕ_{1F}	40.9°		ϕ_{1F}	40.9°	

A. Mixed States

Heavy-light mesons are not charge conjugation eigenstates and so mixing can occur between states with $J = L$ and $S = 0, 1$. For example, the two $J^P = 1^+$ states are a mixture

of n^1P_1 and n^3P_1 states. Thus

$$\begin{aligned} |B(1\ P_1)\rangle &= +\cos(\phi_{1P})|1\ ^1P_1\rangle + \sin(\phi_{1P})|1\ ^3P_1\rangle \\ |B(1\ P'_1)\rangle &= -\sin(\phi_{1P})|1\ ^1P_1\rangle + \cos(\phi_{1P})|1\ ^3P_1\rangle \end{aligned}$$

where ϕ_{1P} is the mixing angle. For D-waves mixing occurs between 3D_2 and 1D_2 states, with a mixing angle denoted as ϕ_{nD} for principal quantum number n . In the heavy quark limit $m_Q \rightarrow \infty$ the mixing angles become[13]

$$\phi_{m_Q \rightarrow \infty} = \arctan\left(\sqrt{\frac{L}{L+1}}\right). \quad (5)$$

This implies $\phi_{1P} = \phi_{2P} = 35.3^\circ$ and $\phi_{1D} = \phi_{2D} = 39.2^\circ$. We have confirmed that these angles are close to those produced by our potential model and hence use them in the subsequent work.

III. STRONG DECAY MODEL

Strong decays will be computed using the 3P_0 model for quark-antiquark pair production. This model dates back to Micu in 1969 [14]; it assumes that quark and antiquarks are produced with vacuum quantum numbers with a strength that is determined by experiment. The model was developed extensively by Le Yaouanc and collaborators[15–17] and applied successfully to many meson decays. The 3P_0 model has also been used to describe baryon decays[16, 18–21] and for diquonia decays to baryon plus antibaryon [22]. Older studies of strong decays considered an alternative phenomenological model in which quark-antiquark pairs are produced with 3S_1 quantum numbers [23, 24]; however, this possibility is disfavoured by measured ratios of partial wave amplitudes [25].

A comprehensive study of light meson strong decays in the 3P_0 model was made by Barnes *et al.* in Ref. [26]. Simple harmonic oscillator (SHO) meson wave functions were used in this work. The same assumptions were used for strong decays in the $n\bar{s}$, $s\bar{s}$, $c\bar{c}$, $c\bar{n}$, $b\bar{n}$, $b\bar{s}$ ($n = u$ or d) sectors [27–30]. We adopt the same approach here, but fit the SHO wavefunction parameter (denoted β in the following) to the wavefunctions obtained above.

The dependence of typical strong decays on the choice of the SHO parameter β for the B meson is illustrated in Fig. 1, which indicates sensitivities of $d\Gamma/d\beta \approx 0.5$ or less.

In Refs.[28, 30] the β parameter was obtained by equating the root mean square (RMS) radius of a harmonic oscillator wavefunction to the RMS radius of the analogous quark

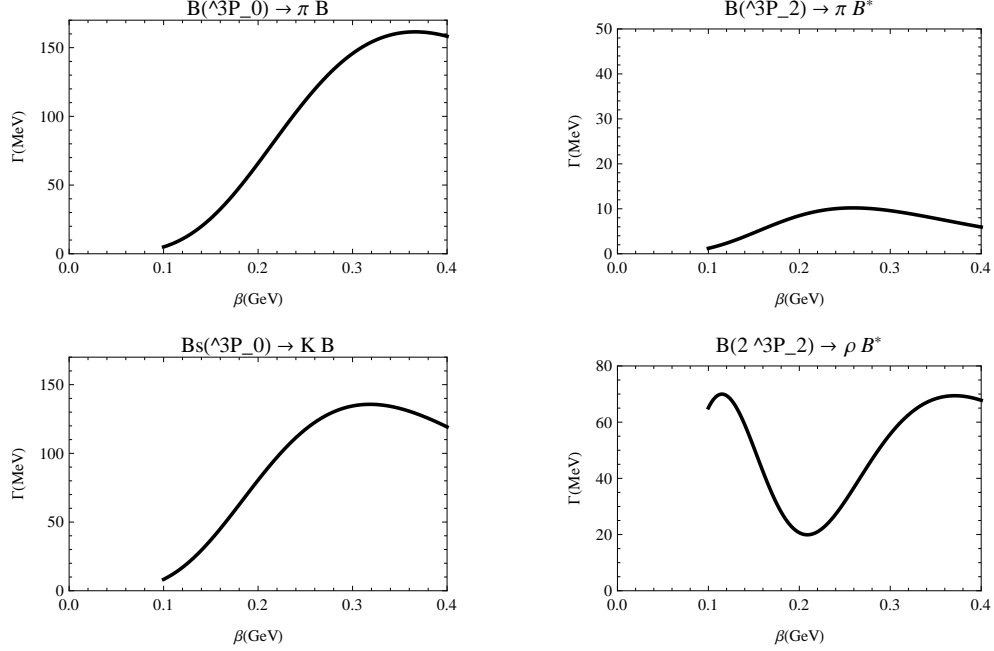


FIG. 1: Partial widths of some of the strong decays of B and B_s mesons in the 3P_0 model are plotted as a function of β for the initial meson.

model wavefunction. In this work we choose to obtain β by fitting the SHO wavefunction to the quark model wavefunction. Typical results are shown in Fig.(2), which compares wavefunctions obtained with all three methods. SHO wavefunction parameters and the error, $\int (U - U_{SHO})^2 dr$, for these cases are reported in Table II. Both methods assume that a typical momentum dominates the decay amplitude with one optimises to the state RMS radius and the other to a global fit to the wavefunction.

TABLE II: Quark model and SHO wavefunction errors, $\int (U - U_{SHO})^2 dr$, for the RMS and fit methods.

Meson	Quantity	By equating rms radius of the realistic and SHO wavefunctions	By fitting β in the SHO form to the realistic wavefunction
$B(1^3S_1)$	$\beta(GeV)$	0.368	0.371
	Error	0.0138	0.0137
$B(2^3S_1)$	$\beta(GeV)$	0.274	0.309
	Error	0.146	0.069
$B(3^3S_1)$	$\beta(GeV)$	0.242	0.273
	Error	0.267	0.090
$B(4^3S_1)$	$\beta(GeV)$	0.225	0.252
	Error	0.398	0.113

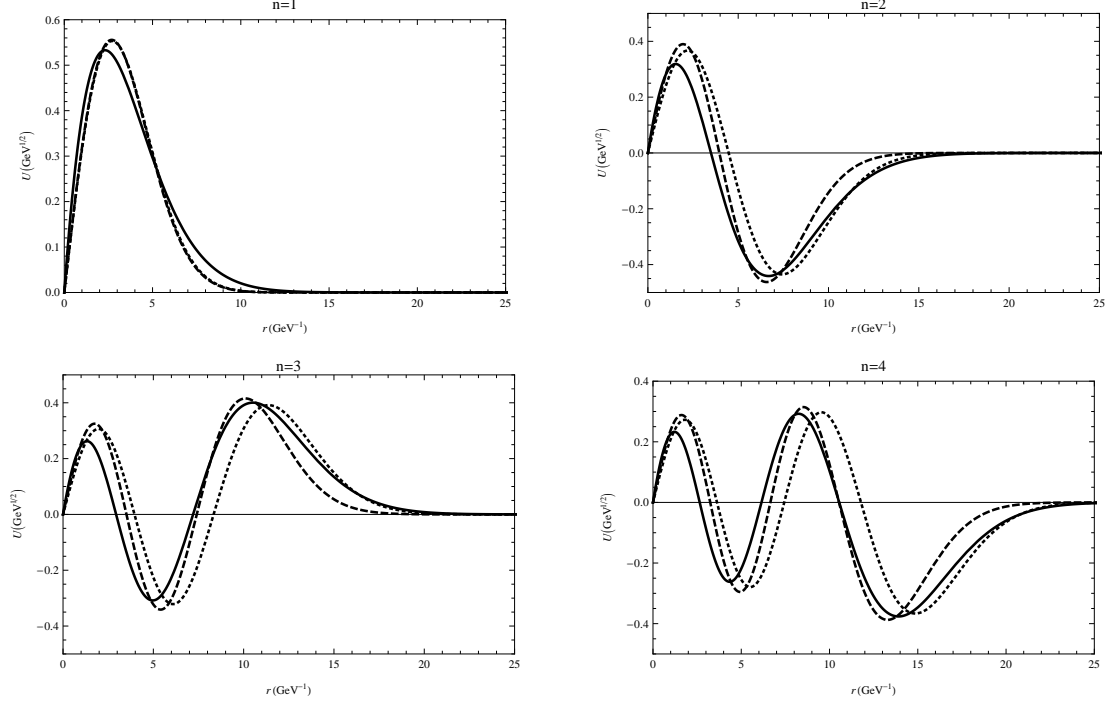


FIG. 2: Radial Wavefunctions of n^3S_1 states of B meson with $n = 1, 2, 3, 4$. Solid: full model, dotted: SHO with RMS β , dashed: SHO with fit β .

With the wavefunctions specified, we now move on to the decay model definition. The interaction Hamiltonian for the 3P_0 model is obtained from the nonrelativistic limit of

$$H_I = 2m_q\gamma \int d^3\mathbf{x} \bar{\psi}_q(\mathbf{x})\psi_q(\mathbf{x}), \quad (6)$$

where γ is a coupling to be determined. The connection with quark-antiquark production can be seen through the familiar second quantized form of the Dirac quark field ψ

$$\psi_q(\mathbf{x}) = \int \frac{d^3\mathbf{k}}{(2\pi)^3} [u(\mathbf{k}, s)b(\mathbf{k}) + v(-\mathbf{k}, s)d^\dagger(-\mathbf{k})] e^{i\mathbf{k}\cdot\mathbf{x}}. \quad (7)$$

In the notation of Eq.(7), quark-antiquark production in an open flavour strong meson decay $A \rightarrow B + C$ is described by the $b^\dagger d^\dagger$ term in H_I of Eq.(6). The pair production strength γ is a dimensionless constant and is determined to be approximately $\gamma = 0.35$ in a fit to the known $c\bar{c}$ states above open-charm threshold[28].

In this paper, we use a modified version of the pair creation strength that replaces γ with

$$\gamma^{\text{eff}} = \frac{m_{u/d}}{m} \gamma,$$

where m is the mass of the produced quark [31–33]. This mechanism suppresses those diagrams in which a heavy $q\bar{q}$ pair is created[33] and is equivalent to fixing the prefactor in Eq. 6 to be $2m_{u/d}$.

To calculate the decay rate of process $A \rightarrow B + C$, we evaluate the matrix element $\langle BC|H_I|A\rangle$ by using quark model $q\bar{q}$ states for the initial and final mesons of the form

$$|A\rangle = |\mathbf{A}; nJM[LS]; II_z\rangle = \int d^3\mathbf{a} d^3\bar{\mathbf{a}} \delta(\mathbf{A} - \mathbf{a} - \bar{\mathbf{a}}) \phi_{nL}\left(\frac{m_{\bar{a}}\mathbf{a} - m_a\bar{\mathbf{a}}}{m_a + m_{\bar{a}}}\right) X_{c,s,f;\bar{c},\bar{s},\bar{f}}^{JM[LS]} Y_{LM_L}(\hat{k}) b_{c,s,f}^\dagger(\mathbf{a}) d_{\bar{c},\bar{s},\bar{f}}^\dagger(\bar{\mathbf{a}}) |0\rangle, \quad (8)$$

where $X_{c,s,f;\bar{c},\bar{s},\bar{f}}^{JM[LS]}$ is a matrix given by

$$X_{c,s,f;\bar{c},\bar{s},\bar{f}}^{JM[LS]} = \frac{\delta_{c\bar{c}}}{\sqrt{3}} \Xi_{f,\bar{f}}^{I,I_z} \langle \frac{1}{2}s, \frac{1}{2}\bar{s} | SM_S \rangle \langle SM_S, LM_L | JM \rangle.$$

A sum over repeated indices is understood in Eq.(8). In the last equation $\Xi_{f,\bar{f}}^{I,I_z}$ is a flavor wavefunction and ϕ is the spatial wavefunction that depends on the momenta \mathbf{a} and $\bar{\mathbf{a}}$ of the quark and antiquark with masses m_a and $m_{\bar{a}}$.

In general four diagrams contribute to each decay amplitude. Two of these correspond to OZI suppressed decays and are disallowed by momentum conservation. The remaining diagrams are shown in Fig.(3). As in Ref. [34], we call the resulting diagram d_1 if the produced quark goes into meson B and d_2 if it goes into meson C .

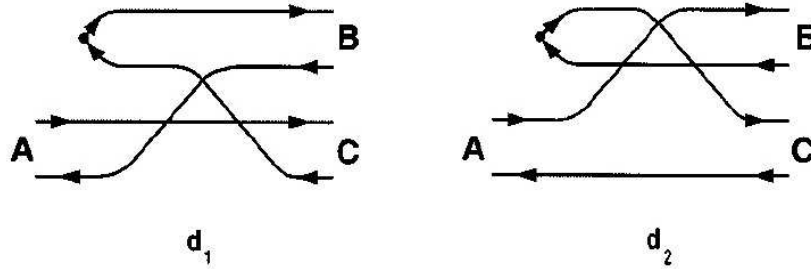


FIG. 3: Decay diagrams in the 3P_0 Model.

The matrix element for each diagram factorises according to

$$\langle BC|H_I|A\rangle = I_{signature} I_{flavour} I_{spin} I_{space}. \quad (9)$$

The first factor is, in the notation of Ref. [34],

$$I_{signature} = \langle 0 | b_c d_{\bar{c}} b_b d_{\bar{b}} b_k^\dagger d_{-\mathbf{k}}^\dagger d_{\bar{a}}^\dagger b_a^\dagger | 0 \rangle, \quad (10)$$

which evaluates to

$$I_{signature} = [\delta(\bar{\mathbf{c}} + \mathbf{k})\delta(\bar{\mathbf{b}} - \bar{\mathbf{a}}) - \delta(\bar{\mathbf{b}} + \mathbf{k})\delta(\bar{\mathbf{c}} - \bar{\mathbf{a}})][\delta(\mathbf{b} - \mathbf{k})\delta(\mathbf{c} - \mathbf{a}) - \delta(\mathbf{c} - \mathbf{k})\delta(\mathbf{b} - \mathbf{a})]. \quad (11)$$

The decay vertex is unity in flavour space, hence the flavour factor $I_{flavour}$ is simply an isospin overlap matrix element. For a decay process having several charge channels (for example $B^+ \rightarrow \pi^+ B^0$ and $B^+ \rightarrow \pi^0 B^+$) the sum over all the charge channels is performed. This is summarised as a multiplicative flavour factor \mathcal{F} . The flavour factor $I_{flavour}(d_1)$ for each process discussed in this paper is zero. For all the processes discussed in this work, $I_{flavor}(d_2)$ and \mathcal{F} are reported in Table III.

Generic Decay	Subprocess	$I_{flavor}(d_2)$	\mathcal{F}
$B \rightarrow \pi B$	$B^+ \rightarrow \pi^+ B^0$	1	3/2
$B \rightarrow \eta B$	$B^+ \rightarrow \eta B^+$	1/2	1
$B \rightarrow \omega B$	$B^+ \rightarrow \omega B^+$	$1/\sqrt{2}$	1
$B \rightarrow \rho B$	$B^+ \rightarrow \rho^+ B^0$	1	3/2
$B \rightarrow KB_s$	$B^+ \rightarrow K^+ B_s^0$	1	1
$B_s \rightarrow KB$	$B_s^0 \rightarrow K^- B^+$	1	2
$B_s \rightarrow \eta B_s$	$B_s^0 \rightarrow \eta B_s^0$	$1/\sqrt{2}$	1

TABLE III: Flavour Factors

Substituting Eqs.(6-8) in $\langle BC|H_I|A\rangle$, we get the (remaining) spin and space factor of the diagram (d_2) for the general process $q_1 \bar{b} \rightarrow q_1 \bar{q}_2 + q_2 \bar{b}$, where q_1 or $q_2 = (u, d, s)$, as

$$I_{spin+space}(d_2) = -2m_q \gamma \int d^3 \mathbf{a} d^3 \bar{\mathbf{a}} d^3 \mathbf{b} d^3 \bar{\mathbf{b}} d^3 \mathbf{c} d^3 \bar{\mathbf{c}} \phi_A \left(\frac{m_b \mathbf{a} - m_{q_1} \bar{\mathbf{a}}}{m_b + m_{q_1}} \right) \delta(\mathbf{A} - \mathbf{a} - \bar{\mathbf{a}}) \\ \cdot \phi_B^* \left(\frac{m_{q_2} \mathbf{b} - m_{q_1} \bar{\mathbf{b}}}{m_{q_1} + m_{q_2}} \right) \delta(\mathbf{B} - \mathbf{b} - \bar{\mathbf{b}}) \phi_C^* \left(\frac{m_b \mathbf{c} - m_{q_2} \bar{\mathbf{c}}}{m_b + m_{q_2}} \right) \delta(\mathbf{C} - \mathbf{c} - \bar{\mathbf{c}}) \\ \cdot \int \frac{d^3 \mathbf{k}}{(2\pi)^3} \delta(\bar{\mathbf{a}} - \bar{\mathbf{c}}) \delta(\mathbf{a} - \mathbf{b}) \delta(\mathbf{k} - \mathbf{c}) \delta(-\mathbf{k} - \bar{\mathbf{b}}) \langle s | \bar{u}(\mathbf{k}, s) v(-\mathbf{k}, s) | \bar{s} \rangle. \quad (12)$$

The matrix element $\langle s | \bar{u}(\mathbf{k}, s) v(-\mathbf{k}, s) | \bar{s} \rangle$ is $\frac{1}{m_q} \langle s | \vec{\sigma} | \bar{s} \rangle \cdot \mathbf{k}$ in the nonrelativistic limit. Here $\langle s | \vec{\sigma} | \bar{s} \rangle$ is a spin matrix element which can be calculated by using Eqs. B14-B16 of Ref. [34].

Performing the integrations gives three expressions of the same form in terms of the spherical components of \mathbf{B} . Rather than calculating each, we compute one of them and use the Wigner-Eckart theorem to find the others.

Setting $\vec{k} = k_z$, $\mathbf{A} = 0$, and $\mathbf{C} = -\mathbf{B}$ gives

$$I_{space}(d_2) = -2\gamma \int \frac{d^3\mathbf{k}}{(2\pi)^3} k_z \phi_A(\mathbf{B} + \mathbf{k}) \phi_B^*\left(\frac{m_{q_2}}{m_{q_1} + m_{q_2}}\mathbf{B} + \mathbf{k}\right) \phi_C^*\left(\mathbf{k} + \frac{m_{q_2}}{m_b + m_{q_2}}\mathbf{B}\right). \quad (13)$$

The three-dimensional SHO wavefunctions appearing in this expression have the form[26, 34]

$$\phi_{nlm}(\mathbf{k}) = (2\pi)^{3/2}(-i)^{2n+l} N_{nlm} k^l Y_{lm}(\hat{k}) L_n^{l+1/2}(\beta^{-2}k^2) e^{-\frac{1}{2}\beta^{-2}k^2}, \quad (14)$$

where β is the SHO parameter, N_{nlm} is a normalization constant, and $L_n^{l+1/2}$ is the associated Legendre polynomial.

Finally, the 3P_0 amplitude can be combined with relativistic phase space to express the decay width for $(A \rightarrow B + C)$ in the form[34]

$$\Gamma_{A \rightarrow BC} = 2\pi \frac{P E_B E_C}{M_A} \sum_{LS} |\mathcal{M}_{LS}|^2, \quad (15)$$

where $P = |\mathbf{B}| = |\mathbf{C}|$, M_A is the mass of the initial meson, and E_B and E_C are the energies of the final mesons B and C respectively. Where available, we use experimental masses[35]; otherwise we employ the theoretical masses of Table I.

The partial wave amplitudes referred to in Eq. 15 are given by

$$\mathcal{M}_{LS} = \sum_{M_L M_S M_B M_C} \langle LM_L SM_S | J_A M_A \rangle \langle J_B M_B J_C M_C | SM_S \rangle \int Y_{LM_L}^*(\hat{B}) \mathcal{M}(\mathbf{B}) d\Omega_B \quad (16)$$

and \mathcal{M} is the decay amplitude of Eq. 9.

IV. RADIATIVE TRANSITIONS OF B AND B_s MESONS

A. E1 Radiative Transitions

E1 radiative transition partial widths are computed with the following expression

$$\Gamma(n^{2S+1}L_J \rightarrow n'^{2S'+1}L'_{J'} + \gamma) = \frac{4}{3} \langle e_Q \rangle^2 \alpha \omega^3 C_{fi} \delta_{SS'} |\langle n'^{2S'+1}L'_{J'} | r | n^{2S+1}L_J \rangle|^2 \frac{E_f}{M_i}, \quad (17)$$

where

$$\langle e_Q \rangle = \frac{m_{\bar{q}} Q - m_q \bar{Q}}{m_q + m_{\bar{q}}}. \quad (18)$$

Here Q and \bar{Q} are the charges of the quark and anti-quark in units of $|e|$, m_q and $m_{\bar{q}}$ are the masses of the quark and anti-quark, α is the fine structure constant, ω is the final photon

energy, M_i is mass of the initial meson, and E_f is the energy of the final state. Finally, the angular matrix element C_{fi} is given by

$$C_{fi} = \max(L, L') (2J' + 1) \left\{ \begin{matrix} L' & J' & S \\ J & L & 1 \end{matrix} \right\}^2.$$

This is the result of Ref. [36] except for our inclusion of the relativistic phase space factor E_f/M_i . The matrix elements $\langle n'^{2S'+1} L'_{J'} | r | n^{2S+1} L_J \rangle$ are obtained via numerical integration over the quark model wavefunctions obtained above.

Wavefunction shifts due to perturbative spin-dependent interactions were neglected in this computation, as with Refs. [28, 29]. Results for E1 radiative transitions for B and B_s mesons are given in Tables IV-XX.

B. M1 Radiative Transitions

The M1 radiative partial widths are evaluated using the following expression[30]

$$\Gamma(n^{2S+1} L_J \rightarrow n'^{2S'+1} L'_{J'} + \gamma) = \frac{\alpha}{3} \omega^3 (2J' + 1) \delta_{S, S' \pm 1} \cdot \left| \frac{e_q}{m_q} \langle f | j_0\left(\frac{m_b}{m_q + m_b} kr\right) | i \rangle + \frac{e_b}{m_b} \langle f | j_0\left(\frac{m_q}{m_q + m_b} kr\right) | i \rangle \right|^2, \quad (19)$$

where ω is the final photon energy and $j_0(x)$ is a spherical Bessel function. The definitions of the other parameters are same as in the E1 radiative transitions. We quote results for M1 radiative transitions for B and B_s mesons in Tables IV-XX.

V. RESULTS AND DISCUSSION

A. B Mesons

Radiative decay rates, strong decay amplitudes, and partial widths for the 1P, 1D, 1F, 2S, 2P, 2D, and 3S B mesons are given in Tables IV-XIII. In these tables $c = \cos \phi_{1P}$ or $\cos \phi_{2P}$, $s = \sin \phi_{1P}$ or $\sin \phi_{2P}$, $c_1 = \cos \phi_{1D}$ or $\cos \phi_{2D}$, and $s_1 = \sin \phi_{1D}$ or $\sin \phi_{2D}$. In the following we will use these results and those of Table I to interpret the recently discovered $B_1(5721)$, $B_2^*(5747)$, and $B_J(5970)$.

1. $B_1(5721)$

In 2016, the LHCb collaboration observed charged and neutral B states, denoted as $B_1(5721)$ [37]. The spin-parity of these states was determined to be $J^P = 1^+$ while their masses are

$$m_{B_1(5721)^+} = 5725.1 \pm 1.8 \pm 3.1 \pm 0.17 \pm 0.4 \text{ MeV}$$

$$m_{B_1(5721)^0} = 5727.7 \pm 0.7 \pm 1.4 \pm 0.17 \pm 0.4 \text{ MeV}.$$

The measured decay widths are

$$\Gamma_{B_1(5721)^+} = 29.1 \pm 3.6 \pm 4.3 \text{ MeV}$$

and

$$\Gamma_{B_1(5721)^0} = 30.1 \pm 1.5 \pm 3.5 \text{ MeV}.$$

Comparison of these mass to our calculated values $m_B(1P_1) = 5755.12 \text{ MeV}$ and $m_B(1P'_1) = 5739.2 \text{ MeV}$ implies that this state is one of the $1P_1$ or $1P'_1$ mesons. The ambiguity is resolved by comparison to the strong widths shown in Table IV, which shows $\Gamma_{B(1P_1)} = 16.4 \text{ MeV}$ and $\Gamma_{B(1P'_1)} = 126.4 \text{ MeV}$. Thus it is likely that the reported state is the narrow member of the $1P$ doublet, namely the $B(1P_1)$.

2. $B_2^*(5747)$

The LHCb collaboration also observed spin partners of the $B_1(5721)$, dubbed $B_2^*(5747)$ [37]. This state has $J^P = 2^+$ and was observed in two charge modes with masses

$$m_{B_2^*(5747)^+} = 5737.2 \pm 0.72 \pm 0.40 \pm 0.17 \text{ MeV},$$

$$m_{B_2^*(5747)^0} = 5739.44 \pm 0.37 \pm 0.33 \pm 0.17 \text{ MeV}$$

and with decay widths of

$$\Gamma_{B_2^*(5747)^+} = 23.6 \pm 2.0 \pm 2.1 \text{ MeV}$$

and

$$\Gamma_{B_2^*(5747)^0} = 24.5 \pm 1.0 \pm 1.5 \text{ MeV}.$$

The measured properties of this state agree very well with the predicted mass and width of the 1^3P_2 state (5767 MeV and 20.4 MeV, respectively). In addition, we obtain the ratio

$$\frac{\Gamma(B_2^*(5747) \rightarrow \pi B^*)}{\Gamma(B_2^*(5747) \rightarrow \pi B)} = 1.002, \quad (20)$$

which is also in good agreement with the experimental measurement[37]:

$$\Gamma(B_2^*(5747)^+ \rightarrow B^{*0}\pi^+)/\Gamma(B_2^*(5747)^+ \rightarrow B^0\pi^+) = 1.0 \pm 0.5 \pm 0.8$$

$$\Gamma(B_2^*(7)^0 \rightarrow B^{*+}\pi^-)/\Gamma(B_2^*(5747)^0 \rightarrow B^+\pi^-) = 0.71 \pm 0.14 \pm 0.3.$$

3. $B_J(5840)$ and $B_J(5970)$

Two "structures" labelled $B_J(5970)$ and $B_J(5840)$ have been reported by CDF[3] and LHCb[4]. Averaging the charge modes yields masses and widths of

$$M(B_J(5840)) = 5857 \pm 21 \text{ MeV} \quad \Gamma(B_J(5840)) = 176 \pm 90 \text{ MeV} \quad (21)$$

and

$$M(B_J(5970)) = 5968 \pm 7 \text{ MeV} \quad \Gamma(B_J(5970)) = 72 \pm 23 \text{ MeV}. \quad (22)$$

The spin and parity of these states is unknown; however, the LHCb collaboration has suggested that the B_J signals be identified with the 2^1S_0 and 2^3S_1 quark model bottom states. The measured masses and widths are difficult to fit with quark models. For example, the Godfrey-Isgur and ARM models of Ref. [30] predict a $2S$ mass splitting of 39 and 30 MeV respectively, while we predict a splitting of 28 MeV. These are substantially less than the measured splitting 111 ± 22 MeV. This observation stands in contrast to the $n = 1$ hyperfine splitting, where the measured difference is 45 MeV and the model predictions are 59 MeV (Godfrey-Isgur), 41 MeV (ARM), and 62 MeV (this work).

In spite of this problem, the $B_J(5840)$ mass is reasonably close to model predictions for the 2^1S_0 state, being 37 MeV below the Godfrey-Isgur result, 23 MeV above the ARM prediction, and 20 MeV above our prediction. However, our predicted width for this state is 16 MeV, fairly low with respect to the measured width of 176 MeV (although with large error). In contrast, the width predicted in Ref. [30] (95 MeV) is in good agreement with experiment. One concludes that identifying the $B_J(5840)$ with the 2^1S_0 quark model state

is reasonable. We note, however, that the $B\pi$ decay mode is reported as "possibly seen" by LHCb [4], which would require dismissing the 2^1S_0 identification if confirmed.

The quark model states closest to the $B_J(5970)$ in mass are the ground state D waves, with masses near 6030 MeV, approximately 60 MeV too high. This is possibly an acceptable error since the B and B_s flavour sectors are rather poorly constrained. The strong decay widths for these states, reported in Table V, range from 34 to 67 MeV. All of these match within errors with the measured width, with preference for the 1^3D_1 or $1D'_2$ states. Again, the $B\pi$ decay is "possibly seen". If this is confirmed then the $1D'_2$ mode is disallowed. Overall, we slightly prefer the 1^3D_1 identification of the $B_J(5970)$.

4. *B meson decay properties*

TABLE IV: Partial widths and branching ratios for strong, E1 and M1 decays of the 1S and 1P states of B mesons. E1 and M1 amplitudes are in units of $(GeV)^{-1}$ and strong decay amplitudes are in units of $(GeV)^{-1/2}$.

State	Mode	Photon energy (MeV)	Amplitude	$\Gamma_{thy}(ub, db)$ MeV	B.R.(ub,db) (%)
$B(1^3S_1)$	$B\gamma$	45.74	$\langle 1^1S_0 j_0(kr \frac{m_{b,q}}{m_q+m_b}) 1^3S_1 \rangle = 0.9930, 0.9961$	0.0009, 0.0003	100
$B(1^3P_0)$	$B^*\gamma$	365.89	$\langle 1^3S_1 r 1^3P_0 \rangle = 3.258$	0.575, 0.175	0.4, 0.12
	πB		$^1S_0 = -0.392$	141.5	~ 100
	total			142.08, 141.7	100
$B(1P_1)$	$B\gamma$	441.51	$\langle 1^1S_0 r 1^1P_1 \rangle = 2.965$	0.448, 0.137	2.73, 0.86
	$B^*\gamma$	399.07	$\langle 1^3S_1 r 1^3P_1 \rangle = 3.258$	0.339, 0.103	2.07, 0.65
	πB^*		$^3S_1 = -0.222c + 0.313s,$ $^3D_1 = -0.109c - 0.077s$	15.62	96.7
	total			16.4, 15.9	100
$B(1P'_1)$	$B\gamma$	456.19	$\langle 1^1S_0 r 1^1P_1 \rangle = 2.965$	0.415, 0.127	0.328, 0.1
	$B^*\gamma$	413.86	$\langle 1^3S_1 r 1^3P_1 \rangle = 3.258$	0.448, 0.137	0.1, 0.11
	πB^*		$^3S_1 = +0.296c + 0.211s,$ $^3D_1 = -0.082c + 0.115s$	125.53	~ 100
	total			126.4, 125.8	100
$B(1^3P_2)$	$B^*\gamma$	402.6	$\langle 1^3S_1 r 1^3P_2 \rangle = 3.258$	0.761, 0.232	3.7, 1.17
	πB		$^1D_2 = +0.094$	9.77	48.7
	πB^*		$^3D_2 = -0.105$	9.79	48.8
	total			20.3, 19.8	100

TABLE V: Partial widths and branching ratios for strong, E1 and M1 decays of the 1D states of B mesons (format as in Table IV).

State	Mode	Photon energy (MeV)	Amplitude	$\Gamma_{thy}(ub, db)$ MeV	B.R.(ub, db) (%)
$B(1^3D_1)$	$B(1^3P_0)\gamma$	310.31	$\langle 1^3P_0 r 1^3D_1 \rangle = 5.399$	0.65,0.199	0.9745,0.3002
	$B(1^3P_2)\gamma$	272.91	$\langle 1^3P_2 r 1^3D_1 \rangle = 5.399$	0.022,0.007	0.033,0.0106
	πB		$^1P_1 = +0.093$	23.22	34.9
	πB^*		$^3P_1 = +0.073$	12.49	18.78
	ηB		$^1P_1 = +0.065$	7.99	12.0
	ηB^*		$^3P_1 = +0.050$	3.87	5.8
	KB_s		$^1P_1 = +0.095$	13.21	19.8
	KB_s^*		$^3P_1 = +0.068$	5.28	7.9
	total			66.7,66.3	100
$B(1^3D_3)$	$B(1^3P_2)\gamma$	280.98	$\langle 1^3P_2 r 1^3D_3 \rangle = 5.399$	0.874,0.267	2.3245,0.7216
	πB		$^1F_3 = +0.076$	15.69	42
	πB^*		$^3F_3 = -0.090$	19.49	52.2
	ηB		$^1F_3 = +0.017$	0.56	1.5
	ηB^*		$^3F_3 = -0.017$	0.44	1.17
	KB_s		$^1F_3 = +0.015$	0.36	0.96
	KB_s^*		$^3F_3 = -0.013$	0.20	0.53
	total			37.6,37.0	100
$B(1D_2)$	$B(1^3P_2)\gamma$	278.63	$\langle 1^3P_2 r 1^3D_2 \rangle = 5.399$	0.212,0.065	0.6127,0.189
	πB^*		$^3P_2 = +0.078c_1 - 0.095s_1,$ $^3F_2 = +0.092c_1 + 0.075s_1$	33.64	97.5
	ηB^*		$^3P_2 = +0.055c_1 - 0.067s_1,$ $^3F_2 = +0.017c_1 + 0.014s_1$	0.74	2.1
	total			34.6,34.4	100
$B(1D_2')$	$B(1^3P_2)\gamma$	279.53	$\langle 1^3P_2 r 1^3D_2 \rangle = 5.399$	0.0011,0.0003	0.002,0.0005
	πB^*		$^3P_2 = -0.095c_1 - 0.077s_1,$ $^3F_2 = +0.075c_1 - 0.092s_1$	36.19	56.11
	ηB^*		$^3P_2 = -0.067c_1 - 0.055s_1,$ $^3F_2 = +0.014c_1 - 0.017s_1$	11.88	18.42
	KB_s^*		$^3P_2 = -0.092c_1 - 0.075s_1,$ $^3F_2 = +0.010c_1 - 0.013s_1$	16.43	25.47
	total			64.5,64.5	100

TABLE VI: Partial widths and branching ratios for strong, E1 and M1 decays of the $1F$ states of B mesons (format as in Table IV).

State	Mode	Photon energy (MeV)	Amplitude	$\Gamma_{thy}(ub, db)$ MeV	B.R.(ub, db) (%)
$B(1^3F_2)$	$B(1^3D_1)\gamma$	232.21	$\langle 1^3D_1 r 1^3F_2 \rangle = 7.076$	0.77,0.235	1.08,0.34
	$B(1D_2)\gamma$	226.45	$\langle 1^3D_2 r 1^3F_2 \rangle = 7.076$	0.71,0.217	1.0,0.31
	$B(1D'_2)\gamma$	225.53	$\langle 1^3D_2 r 1^3F_2 \rangle = 7.076$	0.0035,0.001	0.005,0.001
	$B(1^3D_3)\gamma$	224.16	$\langle 1^3D_3 r 1^3F_2 \rangle = 7.076$	0.004,0.001	0.006,0.001
	πB		$^1D_2 = +0.032$	4.40	6.2
	πB^*		$^3D_2 = +0.028$	3.19	4.5
	ηB		$^1D_2 = +0.022$	1.87	2.6
	ηB^*		$^3D_2 = +0.021$	1.46	2.1
	ρB		$^3D_2 = +0.054$	8.12	11.6
	ρB^*		$^1D_2 = +0.045, ^5D_2 = -0.034, ^5G_2 = -0.095$	28.92	41
	ωB		$^3D_2 = +0.032$	2.77	3.9
	ωB^*		$^1D_2 = +0.026, ^5D_2 = -0.020, ^5G_2 = -0.052$	8.65	12.3
	$\pi B(2^1S_0)$		$^1D_2 = -0.053$	2.14	3.0
	$\pi B(2^3S_1)$		$^3D_2 = -0.041$	1.11	1.6
	KB_s		$^1D_2 = +0.035$	3.98	5.6
	KB_s^*		$^3D_2 = +0.032$	2.92	4.1
	total			71,70	100
$B(1^3F_4)$	$B(1^3D_3)\gamma$	217.33	$\langle 1^3D_3 r 1^3F_4 \rangle = 7.076$	0.753,0.23	0.7591,0.2323
	πB		$^1G_4 = +0.046$	9.18	9.26
	πB^*		$^3G_4 = -0.054$	12.42	12.53
	ηB		$^1G_4 = +0.015$	0.82	0.82
	ηB^*		$^3G_4 = -0.017$	1.01	1.01
	ρB		$^3G_4 = -0.057$	8.92	9
	ρB^*		$^5D_4 = -0.134, ^1G_4 = +0.023, ^5G_4 = -0.045$	46.49	46.9
	ωB		$^3G_4 = -0.032$	2.67	2.69
	ωB^*		$^5D_4 = -0.077, ^1G_4 = +0.012, ^5G_4 = -0.024$	15.03	15.16
	KB_s		$^1G_4 = +0.017$	0.93	0.94
	KB_s^*		$^3G_4 = -0.019$	0.98	0.99
	total			99.2,99	100

TABLE VII: Partial widths and branching ratios for strong, E1 and M1 decays of the 2S states of B mesons (format as in Table IV).

State	Mode	Photon energy (MeV)	Amplitude	$\Gamma_{thy}(ub, db)$ MeV	B.R.(ub,db) (%)
$B(2^1S_0)$	$B^*\gamma$	526.18	$\langle 1^3S_1 j_0(kr \frac{m_{b,q}}{m_q+m_b}) 2^1S_0 \rangle = 0.1985, -0.0695$	0.181, 0.0421	1.1603, 0.2752
	$B(1P_1)\gamma$	136.49	$\langle 1^1P_1 r 2^1S_0 \rangle = -4.4898$	0.096, 0.0294	0.6154, 0.1922
	$B(1P'_1)\gamma$	120.92	$\langle 1^1P_1 r 2^1S_0 \rangle = -4.4898$	0.057, 0.0173	0.3654, 0.1131
	πB^*		$^3P_0 = -0.100$	15.25	~ 100
	total			15.6, 15.3	100
$B(2^3S_1)$	$B\gamma$	592.91	$\langle 1^1S_0 j_0(kr \frac{m_{b,q}}{m_q+m_b}) 2^3S_1 \rangle = 0.2770, 0.0700$	0.161, 0.0423	2.205, 0.613
	$B(2^1S_0)\gamma$	27.98	$\langle 2^1S_0 j_0(kr \frac{m_{b,q}}{m_q+m_b}) 2^3S_1 \rangle = 0.9897, 0.9949$	0.0002, 0.0001	0.003, 0.001
	$B(1^3P_2)\gamma$	160.13	$\langle 1^3P_2 r 2^3S_1 \rangle = -4.3370$	0.148, 0.045	2.027, 0.652
	$B(1P_1)\gamma$	163.82	$\langle 1^3P_1 r 2^3S_1 \rangle = -4.3370$	0.043, 0.0133	0.589, 0.193
	$B(1P'_1)\gamma$	148.33	$\langle 1^3P_1 r 2^3S_1 \rangle = -4.3370$	0.038, 0.012	0.521, 0.174
	$B(1^3P_0)\gamma$	198.27	$\langle 1^3P_0 r 2^3S_1 \rangle = -4.3370$	0.056, 0.017	0.767, 0.246
	πB		$^1P_1 = -0.017$	0.56	7.67, 8.12
	πB^*		$^3P_1 = -0.052$	4.51	61.78, 65.36
	ηB		$^1P_1 = -0.025$	0.64	8.77, 9.28
	ηB^*		$^3P_1 = -0.034$	0.7	9.59, 10.14
	KB_s		$^1P_1 = -0.025$	0.40	5.48, 5.80
	total			7.3, 6.9	100

TABLE VIII: Partial widths and branching ratios for strong, E1 and M1 decays of the 2P states of B mesons (format as in Table IV).

State	Mode	Photon energy (MeV)	Amplitude	$\Gamma_{thy}(ub, db)$ MeV	B.R.(ub, db) (%)
$B(2^3P_0)$	$B^*\gamma$	750.80	$\langle 1^3S_1 r 2^3P_0 \rangle = 0.5734$	0.144,0.044	0.159,0.049
	$B(2^3S_1)\gamma$	219.24	$\langle 2^3S_1 r 2^3P_0 \rangle = 5.21926$	0.327,0.0998	0.361,0.111
	$B(1^3D_1)\gamma$	105.36	$\langle 1^3D_1 r 2^3P_0 \rangle = -4.5973$	0.057,0.018	0.063,0.02
	πB		$^1S_0 = -0.066$	14.72	16.2
	ηB		$^1S_0 = -0.058$	8.88	9.8
	ρB^*		$^1S_0 = +0.138, ^5D_0 = -0.106$	25.99	28.69
	ωB^*		$^1S_0 = +0.090, ^5D_0 = -0.048$	7.61	8.4
	$\pi B(2^1S_0)$		$^1S_0 = -0.175$	9.43	10.41
	KB_s		$^1S_0 = -0.103$	23.45	25.88
	total			90.6,90.2	100
$B(2^3P_2)$	$B^*\gamma$	804.09	$\langle 1^3S_1 r 2^3P_2 \rangle = 0.5734$	0.176,0.054	0.129,0.04
	$B(2^3S_1)\gamma$	277.76	$\langle 2^3S_1 r 2^3P_2 \rangle = 5.21926$	0.659,0.2	0.483,0.147
	$B(1^3D_1)\gamma$	165	$\langle 1^3D_1 r 2^3P_2 \rangle = -4.5973$	0.0022,0.0007	0.002,0.001
	$B(1^3D_3)\gamma$	156.85	$\langle 1^3D_3 r 2^3P_2 \rangle = -4.5973$	0.158,0.048	0.116,0.035
	πB		$^1D_2 = -0.070$	18.58	13.6
	πB^*		$^3D_2 = +0.074$	19.25	14.1
	ηB		$^1D_2 = -0.017$	0.89	0.65
	ηB^*		$^3D_2 = +0.013$	0.47	0.34
	ρB		$^3D_2 = +0.116$	28.62	21
	ρB^*		$^5S_2 = +0.054, ^1D_2 = +0.053, ^5D_2 = -0.014$	41.78	30.6
	ωB		$^3D_2 = +0.067$	9.16	6.7
	ωB^*		$^5S_2 = +0.042, ^1D_2 = +0.030, ^5D_2 = -0.078$	13.76	10.1
	$\pi B(2^1S_0)$		$^1D_2 = -0.035$	0.6	0.44
	$\pi B(2^3S_1)$		$^3D_2 = +0.038$	0.6	0.44
	KB_s		$^1D_2 = -0.022$	1.23	0.9
	KB_s^*		$^3D_2 = +0.016$	0.61	0.45
	total			136.5,136.2	100

TABLE IX: Partial widths and branching ratios for strong, E1 and M1 decays of the 2P states(continued) of B mesons (format as in Table IV).

State	Mode	Photon energy (MeV)	Amplitude	$\Gamma_{thy}(ub, db)$ MeV	B.R.(ub,db) (%)
$B(2P_1)$	$B\gamma$	818.99	$\langle 1^1S_0 r 2^1P_1 \rangle = 0.670513$	0.112,0.0419	0.084,0.031
	$B^*\gamma$	779.46	$\langle 1^3S_1 r 2^3P_1 \rangle = 0.5734$	0.073,0.0224	0.054,0.017
	$B(2^1S_0)\gamma$	277.54	$\langle 2^1S_0 r 2^1P_1 \rangle = 4.84082$	0.307,0.094	0.229,0.07
	$B(2^3S_1)\gamma$	250.72	$\langle 2^3S_1 r 2^3P_1 \rangle = 5.21926$	0.223,0.068	0.166,0.051
	πB^*		$^3S_1 = -0.036c + 0.051s$	25.34	18.9
			$^3D_1 = -0.071c - 0.051s$		
	ηB^*		$^3S_1 = -0.032c + 0.046s$	0.38	0.28
			$^3D_1 = -0.010c - 0.007s$		
	ρB		$^3S_1 = -0.008c + 0.011s$	36.67	27.4
			$^3D_1 = -0.116c - 0.082s$		
	ωB		$^3S_1 = -0.009c + 0.012s$	11.24	8.4
			$^3D_1 = -0.065c - 0.046s$		
	ρB^*		$^3S_1 = 0.069c, ^3D_1 = 0.154c, ^5D_1 = -0.188s$	45.38	33.9
	ωB^*		$^3S_1 = 0.049c, ^3D_1 = 0.084c, ^5D_1 = -0.102s$	13.77	10.3
	KB_s^*		$^3S_1 = -0.058c + 0.082s$	0.51	0.38
			$^3D_1 = -0.013c - 0.009s$		
	total			134,133.5	100
$B(2P'_1)$	$B\gamma$	830.99	$\langle 1^1S_0 r 2^1P_1 \rangle = 0.670513$	0.121,0.037	0.138,0.042
	$B^*\gamma$	791.54	$\langle 1^3S_1 r 2^3P_1 \rangle = 0.5734$	0.091,0.028	0.104,0.032
	$B(2^1S_0)\gamma$	290.74	$\langle 2^1S_0 r 2^1P_1 \rangle = 4.84082$	0.297,0.09	0.338,0.103
	$B(2^3S_1)\gamma$	263.99	$\langle 2^3S_1 r 2^3P_1 \rangle = 5.21926$	0.308,0.094	0.351,0.108
	πB^*		$^3S_1 = +0.046c + 0.033s$	10.89	12.4
			$^3D_1 = -0.053c + 0.074s$		
	ηB^*		$^3S_1 = +0.044c + 0.031s$	7.87	8.96
			$^3D_1 = -0.008c + 0.011s$		
	ρB		$^3S_1 = +0.008c + 0.005s$	0.19	0.22
			$^3D_1 = -0.085c + 0.120s$		
	ωB		$^3S_1 = +0.0002c + 0.0005s$	0.001	0.001
			$^3D_1 = -0.048c + 0.068s$		
	ρB^*		$^3S_1 = -0.102s, ^3D_1 = -0.135s, ^5D_1 = -0.166c$	36.59	41.67
	ωB^*		$^3S_1 = -0.069s, ^3D_1 = -0.072s, ^5D_1 = -0.088c$	10.49	11.95
	KB_s^*		$^3S_1 = +0.080c + 0.056s$	20.99	23.91
			$^3D_1 = -0.011c + 0.015s$		
	total			87.8,87.3	100

TABLE X: Partial widths and branching ratios for strong, E1 and M1 decays of the 2D states of B mesons (format as in Table IV).

State	Mode	Photon energy (MeV)	Amplitude	$\Gamma_{thy}(ub,db)$ MeV	B.R.(ub,db) (%)
$B(2^3D_1)$	$B(1^3P_0)\gamma$	644.45	$\langle 1^3P_0 r 2^3D_1 \rangle = 0.491304$	0.046,0.014	0.0601,0.0183
	$B(1^3P_2)\gamma$	609.16	$\langle 1^3P_2 r 2^3D_1 \rangle = 0.491304$	0.002,0.0006	0.0026,0.0008
	πB		$^1P_1 = -0.016$	1.43	1.87
	πB^*		$^3P_1 = -0.013$	0.83	1.08
	ηB		$^1P_1 = -0.019$	1.79	2.34
	ηB^*		$^3P_1 = -0.015$	1.02	1.33
	ρB		$^3P_1 = -0.031$	3.74	4.89
	ρB^*		$^1P_1 = +0.026, ^5P_1 = -0.012, ^5F_1 = -0.102$	40.11	52.46
	ωB		$^3P_1 = -0.018$	1.25	1.63
	ωB^*		$^1P_1 = +0.015, ^5P_1 = -0.007, ^5F_1 = -0.061$	14.12	18.46
	KB_s		$^1P_1 = -0.041$	6.99	9.14
	KB_s^*		$^3P_1 = -0.032$	3.80	4.97
	K^*B_s		$^3P_1 = -0.022$	1.10	1.43
	$K^*B_s^*$		$^1P_1 = +0.010, ^5P_1 = -0.005, ^5F_1 = -0.006,$	0.28	0.36
	total			76.5,76.4	100
$B(2^3D_3)$	$B(1^3P_2)\gamma$	619.16	$\langle 1^3P_2 r 2^3D_3 \rangle = 0.491304$	0.073,0.0224	0.063,0.019
	πB		$^1F_3 = +0.067$	24.78	21.3
	πB^*		$^3F_3 = -0.076$	29.40	25.3
	ηB		$^1F_3 = +0.024$	2.81	2.42
	ηB^*		$^3F_3 = -0.026$	2.98	2.56
	ρB		$^3F_3 = -0.028$	3.19	2.75
	ρB^*		$^5P_3 = -0.072, ^1F_3 = +0.023, ^5F_3 = -0.050$	30.38	26.14
	ωB		$^3F_3 = -0.017$	1.22	1.06
	ωB^*		$^5P_3 = -0.041, ^1F_3 = +0.014, ^5F_3 = -0.030$	10.25	8.82
	$\pi B(2^1S_0)$		$^1F_3 = +0.018$	0.46	0.4
	$\pi B(2^3S_1)$		$^3F_3 = -0.023$	0.67	0.58
	KB_s		$^1F_3 = +0.031$	4.00	3.44
	KB_s^*		$^3F_3 = -0.032$	3.98	3.43
	K^*B_s		$^3F_3 = -0.0005$	7.20×10^{-4}	0.001
	$K^*B_s^*$		$^5P_3 = -0.032, ^1F_3 = +0.002, ^5F_3 = -0.003$	1.97	1.7
	total			116.2,116.1	100

TABLE XI: Partial widths and branching ratios for strong, E1 and M1 decays of the 2D states(continued) of B mesons (format as in Table IV).

State	Mode	Photon energy (MeV)	Amplitude	$\Gamma_{thy}(ub,db)$ MeV	B.R.(ub,db) (%)
$B(2D_2)$	$B(1^3P_2)\gamma$	615.82	$\langle 1^3P_2 r 2^3D_2\rangle = 0.491304$	0.018,0.005	0.016,0.005
	$B(2^3P_2)\gamma$	198.9	$\langle 2^3P_2 r 2^3D_2\rangle = 7.13132$	0.137,0.042	0.125,0.038
	πB^*		$^3P_2 = +0.013c_1 - 0.016s_1,$ $^3F_2 = +0.078c_1 + 0.064s_1$	50.91	46.6
	ηB^*		$^3P_2 = +0.016c_1 - 0.020s_1,$ $^3F_2 = +0.026c_1 + 0.021s_1$	5.1	4.67
	ρB		$^3P_2 = +0.033c_1 - 0.041s_1,$ $^3F_2 = +0.030c_1 + 0.025s_1$	6.11	5.6
	ωB		$^3P_2 = +0.019c_1 - 0.024s_1,$ $^3F_2 = +0.019c_1 + 0.015s_1$	2.31	2.1
	ρB^*		$^3P_2 = -0.051c_1, ^3F_2 = -0.068c_1,$ $^5P_2 = +0.036s_1, ^5F_2 = +0.078s_1$	26.55	24.3
	ωB^*		$^3P_2 = -0.029c_1, ^3F_2 = -0.041c_1,$ $^5P_2 = +0.021s_1, ^5F_2 = +0.047s_1$	9.25	8.5
	$\pi B(2^3S_1)$		$^3P_2 = +0.009c_1 - 0.104s_1,$ $^3F_2 = +0.024c_1 + 0.019s_1$	1.17	1.1
	KB_s^*		$^3P_2 = +0.034c_1 - 0.041s_1,$ $^3F_2 = +0.033c_1 + 0.027s_1$	6.85	6.3
	K^*B_s		$^3P_2 = +0.025c_1 - 0.030s_1,$ $^3F_2 = +0.0006c_1 + 0.0005s_1$	0.002	0.002
	$K^*B_s^*$		$^3P_2 = -0.022c_1, ^3F_2 = -0.004c_1,$ $^5P_2 = +0.016s_1, ^5F_2 = +0.005s_1$	0.76	0.7
	total			109.2,109.1	100

TABLE XII: Partial widths and branching ratios for strong, E1 and M1 decays of the 2D states(continued) of B mesons (format as in Table IV).

State	Mode	Photon energy (<i>MeV</i>)	Amplitude	$\Gamma_{thy}(ub, db)$ <i>MeV</i>	B.R(<i>ub,db</i>) (%)
$B(2D_2')$	$B(1^3P_2)\gamma$	616.27	$\langle 1^3P_2 r 2^3D_2 \rangle = 0.491304$	0.0001,0.00003	0.0001,0.00004
	$B(2^3P_2)\gamma$	199.38	$\langle 2^3P_2 r 2^3D_2 \rangle = 7.13132$	0.001,0.0002	0.0014,0.00028
	πB^*		$^3P_2 = -0.016c_1 - 0.013s_1,$ $^3F_2 = +0.064c_1 - 0.078s_1$	2.08	2.88
	ηB^*		$^3P_2 = -0.020c_1 - 0.016s_1,$ $^3F_2 = +0.021c_1 - 0.026s_1$	2.87	3.97
	ρB		$^3P_2 = -0.041c_1 - 0.033s_1,$ $^3F_2 = +0.024c_1 - 0.030s_1$	11.23	15.53
	ωB		$^3P_2 = -0.024c_1 - 0.019s_1,$ $^3F_2 = +0.015c_1 - 0.018s_1$	3.76	5.2
	ρB^*		$^3P_2 = +0.051s_1, ^3F_2 = +0.069s_1,$ $^5P_2 = +0.036c_1, ^5F_2 = +0.080c_1$	27.2	37.62
	ωB^*		$^3P_2 = +0.029s_1, ^3F_2 = +0.042s_1,$ $^5P_2 = +0.021c_1, ^5F_2 = +0.048c_1$	9.51	13.15
	$\pi B(2^3S_1)$		$^3P_2 = -0.011c_1 - 0.009s_1,$ $^3F_2 = +0.019c_1 - 0.024s_1$	0.25	0.35
	$K^* B_s$		$^3P_2 = -0.030c_1 - 0.025s_1,$ $^3F_2 = +0.0006c_1 - 0.0007s_1$	3.64	5.03
	KB_s^*		$^3P_2 = -0.042c_1 - 0.034s_1,$ $^3F_2 = +0.027c_1 - 0.032s_1$	11.12	15.38
	$K^* B_s^*$		$^3P_2 = +0.021s_1, ^3F_2 = +0.004s_1,$ $^5P_2 = +0.015c_1, ^5F_2 = +0.005c_1$	0.62	0.86
	total			72.3,72.3	100

TABLE XIII: Partial widths and branching ratios for strong, E1 and M1 decays of the 3S states of B mesons (format as in Table IV).

State	Mode	Photon energy (MeV)	Amplitude	$\Gamma_{thy}(ub, db)$ MeV	B.R.(ub,db) (%)
$B(3^1S_0)$	$B^*\gamma$	889.07	$\langle 1^3S_1 j_0(kr \frac{m_{b,q}}{m_q+m_b}) 3^1S_0 \rangle = 0.17019, -0.03307$	0.633, 0.152	2.38, 0.587
	$B(2^3S_1)\gamma$	370.98	$\langle 2^3S_1 j_0(kr \frac{m_{b,q}}{m_q+m_b}) 3^1S_0 \rangle = 0.24297, -0.05789$	0.094, 0.022	0.353, 0.085
	$B(1P_1)\gamma$	524.83	$\langle 1^1P_1 r 3^1S_0 \rangle = 0.195518$	0.01, 0.003	0.038, 0.012
	$B(1P'_1)\gamma$	510.28	$\langle 1^1P_1 r 3^1S_0 \rangle = 0.195518$	0.008, 0.002	0.03, 0.008
	$B(2P_1)\gamma$	125.31	$\langle 2^1P_1 r 3^1S_0 \rangle = -6.90827$	0.177, 0.054	0.665, 0.208
	$B(2P'_1)\gamma$	111.72	$\langle 2^1P_1 r 3^1S_0 \rangle = -6.90827$	0.106, 0.032	0.398, 0.124
	πB^*		$^3P_0 = +0.027$	3.12	11.73
	ηB^*		$^3P_0 = +0.008$	0.23	0.88
	ρB		$^3P_0 = +0.022$	1.49	5.6
	ρB^*		$^3P_0 = +0.022$	1.23	4.62
	ωB		$^3P_0 = +0.010$	0.30	1.13
	ωB^*		$^3P_0 = +0.018$	0.85	3.2
	$\pi B(2^3S_1)$		$^3P_0 = -0.053$	2.12	7.97
	$\pi B(1^3P_0)$		$^1S_0 = +0.086$	13.46	50.6
	$\pi B(1^3P_2)$		$^5D_0 = -0.033$	1.65	6.2
	KB_s^*		$^3P_0 = +0.016$	0.76	2.86
	K^*B_s		$^3P_0 = +0.009$	0.08	0.3
	$KB_s(1^3P_0)$		$^1S_0 = -0.027$	0.33	1.24
	total			26.6, 26	100
$B(3^3S_1)$	$B\gamma$	945.03	$\langle 1^1S_0 j_0(kr \frac{m_{b,q}}{m_q+m_b}) 3^3S_1 \rangle = 0.19328, 0.03665$	0.319, 0.0828	0.979, 0.258
	$B(2^1S_0)\gamma$	416.18	$\langle 2^1S_0 j_0(kr \frac{m_{b,q}}{m_q+m_b}) 3^3S_1 \rangle = 0.27629, 0.0587$	0.056, 0.0145	0.172, 0.045
	$B(3^1S_0)\gamma$	20.20	$\langle 3^1S_0 j_0(kr \frac{m_{b,q}}{m_q+m_b}) 3^3S_1 \rangle = 0.99, 0.99549$	0.0001, 0.00002	0.0003, 0.0001
	$B(1^3P_2)\gamma$	539.89	$\langle 1^3P_2 r 3^3S_1 \rangle = 0.06559$	0.0012, 0.0004	0.004, 0.001
	$B(1P_1)\gamma$	543.35	$\langle 1^3P_1 r 3^3S_1 \rangle = 0.06559$	0.0003, 0.0001	0.001, 0.0003
	$B(1P'_1)\gamma$	528.84	$\langle 1^3P_1 r 3^3S_1 \rangle = 0.06559$	0.00037, 0.0001	0.001, 0.0003
	$B(1^3P_0)\gamma$	575.60	$\langle 1^3P_0 r 3^3S_1 \rangle = 0.06559$	0.0003, 0.0001	0.001, 0.0003
	$B(2^3P_2)\gamma$	117.45	$\langle 2^3P_2 r 3^3S_1 \rangle = -6.69759$	0.14, 0.0428	0.429, 0.1333
	$B(2P_1)\gamma$	145.10	$\langle 2^3P_1 r 3^3S_1 \rangle = -6.69759$	0.072, 0.0221	0.221, 0.0688
	$B(2P'_1)\gamma$	131.56	$\langle 2^3P_1 r 3^3S_1 \rangle = -6.69759$	0.064, 0.0196	0.196, 0.0611
	$B(2^3P_0)\gamma$	176.99	$\langle 2^3P_0 r 3^3S_1 \rangle = -6.69759$	0.095, 0.029	0.291, 0.0903
	πB		$^1P_1 = +0.033$	5.16	15.83, 16.07
	πB^*		$^3P_1 = +0.034$	5.19	15.92, 16.17
	ηB		$^1P_1 = +0.003$	0.05	0.15, 0.16
	ηB^*		$^3P_1 = +0.002$	0.01	0.03, 0.03
	ρB		$^3P_1 = +0.035$	3.98	12.21, 12.4
	ρB^*		$^1P_1 = -0.005, ^5P_1 = +0.023$	1.56	4.79, 4.86
	ωB		$^3P_1 = +0.018$	1.10	3.37, 3.43
	ωB^*		$^1P_1 = -0.002, ^5P_1 = +0.008$	0.20	0.61, 0.62
	$\pi B(2^1S_0)$		$^1P_1 = +0.014$	0.2	0.61, 0.62
	$\pi B(2^3S_1)$		$^3P_1 = -0.030$	0.76	2.33, 2.37
	$\pi B(1P_1)$		$^3S_1 = +0.072c + 0.052s$	13.01	39.91, 40.53
			$^3D_1 = +0.008c - 0.010s$		
	$\pi B(1P'_1)$		$^3S_1 = -0.052c + 0.073s$	0.15	0.46, 0.47
			$^3D_1 = +0.007c + 0.006s$		
	$\pi B(1^3P_2)$		$^5D_1 = -0.014$	0.31	0.95, 0.97
	KB_s		$^1P_1 = +0.001$	0.01	0.03, 0.03
	KB_s^*		$^3P_1 = +0.007$	0.17	0.52, 0.53
	total			32.6, 32.1	100

B. B_s Mesons

Strong decay amplitudes, radiative transitions, and partial widths for the 1P, 1D, 1F, 2S, 2P, and 2D B_s mesons are given in Tables XVI-XX. In these tables $c = \cos \phi_{1P}$ or $\cos \phi_{2P}$, $s = \sin \phi_{1P}$ or $\sin \phi_{2P}$, $c_1 = \cos \phi_{1D}$ or $\cos \phi_{2D}$, $s_1 = \sin \phi_{1D}$ or $\sin \phi_{2D}$. These results are used to interpret the observed mesons $B_{s1}(5830)$ and $B_{s2}^*(5840)$.

1. $B_{s1}(5830)$

The CDF collaboration observed a bottom-strange state, called the $B_{s1}(5830)$, with $J^P = 1^+$ and mass[3]:

$$m_{B_{s1}(5830)} = 5828.3 \pm 0.1 \pm 0.2 \pm 0.4 \text{ MeV}.$$

The width of this state was determined to be

$$\Gamma_{B_{s1}(5830)} = 0.5 \pm 0.3 \pm 0.3 \text{ MeV}.$$

Evidently this state is one of the $1P_1$ doublet mesons, which have predicted masses near 5800 MeV. These masses are just above BK threshold and therefore small widths are predicted for the narrow $1P_1$ and (nominally) wide $1P_1'$ states. Because of this no further identification can be made.

2. $B_{s2}^*(5840)$

The CDF collaboration has also reported the $B_{s2}^*(5840)$ [3]. This is a $J^P = 2^+$ state of mass

$$m_{B_{s2}^*(5840)} = 5839.7 \pm 0.1 \pm 0.1 \pm 0.2 \text{ MeV}$$

and width

$$\Gamma_{B_{s2}^*(5840)} = 1.4 \pm 0.4 \pm 0.2 \text{ MeV}.$$

These values compare favourably with the predicted mass $m_{B_s}(1^3P_2) = 5821.53 \text{ MeV}$ and width $\Gamma_{B_s}(1^3P_2) = 1.9 \text{ MeV}$. In addition, we also obtain the ratio

$$\frac{\Gamma(B_{s2}^*(5840) \rightarrow KB^*)}{\Gamma(B_{s2}^*(5840) \rightarrow KB)} = 0.084, \quad (23)$$

which is also in good agreement with the experimental measurement[2]

$$\Gamma(B_{s2}^*(5840) \rightarrow B^{*+}K^-)/\Gamma(B_{s2}^*(5840) \rightarrow B^+K^-) = 0.093 \pm 0.013 \pm 0.012.$$

3. Comparison to Other Work

A summary of observables related to the recently observed B and B_s mesons and our predictions is presented in Table XIV. This table also shows related predictions from Ref. [30]. This work suggests that the $B_J(5970)$ could be 2^3S_1 state with a predicted width of 107.8 MeV. We have rather assigned this meson to the 1^3D_1 state

TABLE XIV: Comparison of theoretical and experimental decay widths of observed B and B_s states. Experimental decay widths are taken from PDG [35], ratios of B and B_s states are taken from LHCb [37] and [2] respectively. Decay modes in brackets are "possibly seen".

State	Observed decays	Measured Γ (MeV)	Our predicted Γ (MeV)	Ref. [30] Γ (MeV)
$B_1(5721)^+$	$B^{*0}\pi^+$	31 ± 6	16.4	7.27
$B_1(5721)^0$	$B^{*+}\pi^-$	27.5 ± 3.4		
$B_2^*(5747)^+$	$B^0\pi^+, B^{*0}\pi^+$	20 ± 5	20.3	11.71
$B_2^*(5747)^0$	$B^+\pi^-, B^{*+}\pi^-$	24.2 ± 1.7		
	$\Gamma(B_2^{*+} \rightarrow B^{*0}\pi^+)/\Gamma(B_2^{*+} \rightarrow B^0\pi^+)$	$1.0 \pm 0.5 \pm 0.8$	1.002	0.809
	$\Gamma(B_2^{*0} \rightarrow B^{*+}\pi^-)/\Gamma(B_2^{*0} \rightarrow B^+\pi^-)$	$0.71 \pm 0.14 \pm 0.3$		
$B_J(5840)^+$	$[B^0\pi^+], B^{*0}\pi^+$	224 ± 80	16	95
$B_J(5840)^0$	$[B^+\pi^-], B^{*+}\pi^-$	127 ± 40		
$B_J(5970)^+$	$[B^0\pi^+], B^{*0}\pi^+$	62 ± 20	66.7	107.8
$B_J(5970)^0$	$[B^+\pi^-], B^{*+}\pi^-$	81 ± 12		
$B_{s1}(5830)^0$	$B^{*+}K^-$	0.5 ± 0.4	kinematically excluded no strong decay	
$B_{s2}^*(5840)^0$	B^+K^-	1.47 ± 0.33	1.9	0.777
	$\Gamma(B_{s2}^{*0} \rightarrow B^{*+}K^-)/\Gamma(B_{s2}^{*0} \rightarrow B^+K^-)$	$0.093 \pm 0.013 \pm 0.012$	0.084	0.012

4. B_s meson decay propertiesTABLE XV: Partial widths and branching ratios for strong, E1 and M1 decays of the 1S and 1P states of B_s mesons (format as in Table IV).

State	Mode	Photon energy (MeV)	Amplitude	Γ_{thy} MeV	B.R (%)
B_s^*	$B_s\gamma$	48.41	$\langle 1^1S_0 j_0(kr \frac{m_{b,s}}{m_s+m_b}) 1^3S_1 \rangle = 0.99469, 0.9976$	0.0002	100
$B_s(1^3P_0)$	$B_s^*\gamma$	343.4	$\langle 1^3S_1 r 1^3P_0 \rangle = 3.0211$	0.133	0.0979
	KB		$^1S_0 = -0.764$	135.66	~ 100
	total			135.8	100
$B_s(1^3P_2)$	$B_s^*\gamma$	409.13	$\langle 1^3S_1 r 1^3P_2 \rangle = 3.0211$	0.225	11.84
	KB		$^1D_2 = -0.044$	1.55	81.57
	KB^*		$^3D_2 = +0.018$	0.13	6.84
	total			1.9	100

TABLE XVI: Partial widths and branching ratios for strong, E1 and M1 decays of the 1D state of B_s mesons (format as in Table IV).

State	Mode	Photon energy (MeV)	Amplitude	Γ_{thy} MeV	B.R (%)
$B_s(1^3D_1)$	$B_s(1^3P_0)\gamma$	280.33	$\langle 1^3P_0 r 1^3D_1 \rangle = 4.99789$	0.126	0.1041
	$B_s(1P_1)\gamma$	249.81	$\langle 1^3P_1 r 1^3D_1 \rangle = 4.99789$	0.031	0.0256
	$B_s(1P'_1)\gamma$	223.82	$\langle 1^3P_1 r 1^3D_1 \rangle = 4.99789$	0.0264	0.0218
	$B_s(1^3P_2)\gamma$	212.98	$\langle 1^3P_2 r 1^3D_1 \rangle = 4.99789$	0.003	0.0025
	KB		$^1P_1 = -0.174$	69.8	57.65
	KB^*		$^3P_1 = +0.135$	36.27	29.96
	ηB_s		$^1P_1 = -0.085$	10.70	8.8
	ηB_s^*		$^3P_1 = +0.060$	4.11	3.39
	total			121.06	100
$B_s(1^3D_3)$	$B_s(1^3P_2)\gamma$	218.87	$\langle 1^3P_2 r 1^3D_3 \rangle = 4.99789$	0.109	0.5
	KB		$^1F_3 = +0.067$	10.64	48.8
	KB^*		$^3F_3 = -0.072$	10.45	47.9
	ηB_s		$^1F_3 = +0.017$	0.44	2.01
	ηB_s^*		$^3F_1 = -0.013$	0.19	0.87
	total			21.8	100
$B_s(1D_2)$	$B_s(1^3P_2)\gamma$	217.22	$\langle 1^3P_2 r 1^3D_2 \rangle = 4.99789$	0.027	0.1452
	KB^*		$^3P_2 = +0.147c_1 - 0.180s_1,$ $^3F_2 = +0.073c_1 + 0.060s_1$	17.89	96.18
	ηB_s^*		$^3P_2 = +0.067c_1 - 0.106s_1,$ $^3F_2 = +0.013c_1 + 0.013s_1$	0.66	3.54
	total			18.6	100
$B_s(1D'_2)$	$B_s(1^3P_2)\gamma$	218.13	$\langle 1^3P_2 r 1^3D_2 \rangle = 4.99789$	0.0001	0.0001
	KB^*		$^3D_2 = -0.180c_1 - 0.146s_1,$ $^3F_2 = +0.060c_1 - 0.073s_1$	108.4	85.69
	ηB_s^*		$^3D_2 = -0.106c_1 - 0.067s_1,$ $^3F_2 = +0.014c_1 - 0.013s_1$	18.13	14.33
	total			126.5	100

TABLE XVII: Partial widths and branching ratios for strong, E1 and M1 decays of the 1F state of B_s mesons (format as in Table IV).

State	Mode	Photon energy (MeV)	Amplitude	Γ_{thy} MeV	B.R (%)
$B_s(1^3F_2)$	$B_s(1^3D_1)\gamma$	212.64	$\langle 1^3D_1 r 1^3F_2\rangle = 6.54008$	0.155	0.2712
	$B_s(1D_2)\gamma$	208.39	$\langle 1^3D_2 r 1^3F_2\rangle = 6.54008$	0.027	0.0472
	$B_s(1D'_2)\gamma$	207.48	$\langle 1^3D_2 r 1^3F_2\rangle = 6.54008$	0.00013	0.0002
	$B_s(1^3D_3)\gamma$	206.74	$\langle 1^3D_3 r 1^3F_2\rangle = 6.54008$	0.0008	0.0014
	KB		$^1D_2 = -0.067$	17.74	31.04
	KB^*		$^3D_2 = -0.061$	13.47	23.57
	K^*B		$^3D_2 = -0.081$	13.75	24.05
	K^*B^*		$^1D_2 = +0.044, ^5D_2 = -0.033, ^5G_2 = -0.014$	4.73	8.27
	ηB_s		$^1D_2 = -0.037$	4.22	7.38
	ηB_s^*		$^3D_2 = -0.033$	3.06	5.35
	total			57.15	100
$B_s(1^3F_4)$	$B_s(1^3D_3)\gamma$	200.54	$\langle 1^3D_3 r 1^3F_4\rangle = 6.54008$	0.155	0.3444
	KB		$^1G_4 = +0.051$	10.34	22.97
	KB^*		$^3G_4 = -0.060$	12.79	28.4
	K^*B		$^3G_4 = -0.016$	0.51	1.1333
	K^*B^*		$^5D_4 = -0.117, ^1G_4 = +0.003, ^5G_4 = -0.006$	18.73	41.6
	ηB_s		$^1G_4 = +0.021$	1.30	2.89
	ηB_s^*		$^3G_4 = -0.021$	1.19	2.64
	total			45	100

TABLE XVIII: Partial widths and branching ratios for strong, E1 and M1 decays of the 2S state of B_s mesons (format as in Table IV).

State	Mode	Photon energy (MeV)	Amplitude	Γ_{thy} MeV	B.R (%)
$B_s(2^1S_0)$	$B_s^*\gamma$	491.06	$\langle 1^3S_1 j_0(kr \frac{m_{b,s}}{m_s+m_b}) 2^1S_0 \rangle = 0.16581, -0.053989$	0.014	0.0358
	$B_s(1P_1)\gamma$	125.69	$\langle 1^1P_1 r 2^1S_0 \rangle = -4.11746$	0.019	0.0486
	$B_s(1P_1')\gamma$	99.1	$\langle 1^1P_1 r 2^1S_0 \rangle = -4.11746$	0.008	0.0205
	KB^*		$^3P_0 = -0.267$	39.03	~ 100
	total			39.1	100
$B_s(2^3S_1)$	$B_s\gamma$	553.69	$\langle 1^1S_0 j_0(kr \frac{m_{b,s}}{m_s+m_b}) 2^3S_1 \rangle = 0.24969, 0.056964$	0.0167	0.0407
	$B_s(2^1S_0)\gamma$	20.24	$\langle 2^1S_0 j_0(kr \frac{m_{b,s}}{m_s+m_b}) 2^3S_1 \rangle = 0.9946, 0.99686$	0.00001	~ 0
	$B_s(1^3P_2)\gamma$	107.99	$\langle 1^3P_2 r 2^3S_1 \rangle = -4.00934$	0.0119	0.029
	$B_s(1P_1)\gamma$	145.5	$\langle 1^3P_1 r 2^3S_1 \rangle = -4.00934$	0.008	0.0195
	$B_s(1P_1')\gamma$	119.03	$\langle 1^3P_1 r 2^3S_1 \rangle = -4.00934$	0.005	0.0122
	$B_s(1^3P_0)\gamma$	176.57	$\langle 1^3P_0 r 2^3S_1 \rangle = -4.00934$	0.01	0.0244
	KB		$^1P_1 = +0.118$	10.74	26.19
	KB^*		$^3P_1 = +0.203$	25.49	62.17
	ηB_s		$^1P_1 = +0.052$	2.72	6.6
	ηB_s^*		$^3P_1 = +0.059$	2.07	5.04
	total			41	100

TABLE XIX: Partial widths and branching ratios for strong, E1 and M1 decays of the 2P state of B_s mesons (format as in Table IV).

State	Mode	Photon energy (MeV)	Amplitude	Γ_{thy} MeV	B.R (%)
$B_s(2^3P_0)$	$B_s^*\gamma$	699.23	$\langle 1^3S_1 r 2^3P_0 \rangle = 0.528051$	0.031	0.0449
	$B_s(2^3S_1)\gamma$	207.03	$\langle 2^3S_1 r 2^3P_0 \rangle = 4.82565$	0.072	0.1042
	$B_s(1^3D_1)\gamma$	101.9	$\langle 1^3D_1 r 2^3P_0 \rangle = -4.24042$	0.014	0.0203
	KB		$^1S_0 = -0.144$	63.90	92.47
	ηB_s		$^1S_0 = -0.047$	5.09	7.36
	total			69.1	100
$B_s(2P_1)$	$B_s\gamma$	768.11	$\langle 1^1S_0 r 2^1P_1 \rangle = 0.60031$	0.028	0.5469
	$B_s^*\gamma$	725.75	$\langle 1^3S_1 r 2^3P_1 \rangle = 0.52805$	0.016	0.3125
	$B_s(2^1S_0)\gamma$	255.39	$\langle 2^1S_0 r 2^1P_1 \rangle = 4.5595$	0.065	1.2695
	$B_s(2^3S_1)\gamma$	235.94	$\langle 2^3S_1 r 2^3P_1 \rangle = 4.8256$	0.048	0.9375
	KB^*		$^3S_1 = -0.082c + 0.115s$	2.71	52.9
			$^3D_1 = -0.024c - 0.018s$		
	ηB_s^*		$^3S_1 = -0.027c + 0.049s$	2.25	43.9
			$^3D_1 = -0.024c - 0.021s$		
	total			5.12	100
$B_s(2P_1')$	$B_s\gamma$	771.09	$\langle 1^1S_0 r 2^1P_1 \rangle = 0.60031$	0.024	0.0359
	$B_s^*\gamma$	729.11	$\langle 1^3S_1 r 2^3P_1 \rangle = 0.52805$	0.019	0.0284
	$B_s(2^1S_0)\gamma$	258.65	$\langle 2^1S_0 r 2^1P_1 \rangle = 4.5595$	0.057	0.0852
	$B_s(2^3S_1)\gamma$	239.21	$\langle 2^3S_1 r 2^3P_1 \rangle = 4.8256$	0.06	0.0897
	KB^*		$^3S_1 = +0.117c + 0.083s$	60.28	90.1
			$^3D_1 = -0.018c + 0.023s$		
	ηB_s^*		$^3S_1 = +0.049c + 0.026s$	6.46	9.65
			$^3D_1 = -0.021c + 0.024s$		
	total			66.9	100
$B_s(2^3P_2)$	$B_s^*\gamma$	742.3	$\langle 1^3S_1 r 2^3P_2 \rangle = 0.52805$	0.036	0.309
	$B_s(2^3S_1)\gamma$	253.97	$\langle 2^3S_1 r 2^3P_2 \rangle = 4.8256$	0.132	1.133
	$B_s(1^3D_1)\gamma$	149.67	$\langle 1^3D_1 r 2^3P_2 \rangle = -4.2404$	0.0004	0.0034
	$B_s(1^3D_3)\gamma$	143.71	$\langle 1^3D_3 r 2^3P_2 \rangle = -4.2404$	0.032	0.2747
	KB		$^1D_2 = -0.041$	5.91	50.72
	KB^*		$^3D_2 = +0.030$	2.65	22.7
	K^*B		$^3D_2 = +0.037$	1.62	13.9
	ηB_s		$^1D_2 = -0.011$	0.29	2.48
	ηB_s^*		$^3D_2 = +0.021$	0.98	8.4
	total			11.65	100

TABLE XX: Partial widths and branching ratios for strong, E1 and M1 decays of the 2D state of B_s mesons (format as in Table IV).

State	Mode	Photon energy (MeV)	Amplitude	Γ_{thy} MeV	B.R (%)
$B_s(2^3D_1)$	$B_s(1^3P_0)\gamma$	590.32	$\langle 1^3P_0 r 2^3D_1 \rangle = 0.44889$	0.009	0.0157
	$B_s(1^3P_2)\gamma$	526.48	$\langle 1^3P_2 r 2^3D_1 \rangle = 0.44889$	0.0003	0.0005
	KB		$^1P_1 = -0.058$	16.60	28.86
	KB^*		$^3P_1 = +0.045$	9.29	16.15
	K^*B		$^3P_1 = +0.057$	11.02	19.16
	K^*B^*		$^1P_1 = +0.038, ^5P_1 = -0.041, ^5F_1 = -0.048$	15.81	27.49
	ηB_s		$^1P_1 = -0.028$	3.11	5.4
	ηB_s^*		$^3P_1 = +0.021$	1.67	2.9
	total			57.5	100
$B_s(2^3D_3)$	$B_s(1^3P_2)\gamma$	534.19	$\langle 1^3P_2 r 2^3D_3 \rangle = 0.44889$	0.012	0.0147
	KB		$^1F_3 = +0.066$	21.65	26.6
	KB^*		$^3F_3 = -0.069$	21.84	26.83
	K^*B		$^3F_3 = -0.007$	0.15	0.18
	K^*B^*		$^5P_3 = -0.108, ^1F_3 = +0.011, ^5F_3 = -0.024$	36.79	45.2
	ηB_s		$^1F_3 = +0.012$	0.63	0.77
	ηB_s^*		$^3F_1 = -0.009$	0.31	0.38
	total			81.38	100
$B_s(2D_2)$	$B_s(1^3P_2)\gamma$	531.58	$\langle 1^3P_2 r 2^3D_2 \rangle = 0.44889$	0.003	0.0079
	$B_s(2^3P_2)\gamma$	184.6	$\langle 2^3P_2 r 2^3D_2 \rangle = 6.5948$	0.029	0.0759
	KB^*		$^3P_2 = +0.048c_1 - 0.059s_1,$ $^3F_2 = +0.070c_1 + 0.057s_1$	37.47	98.09
	ηB_s^*		$^3P_2 = +0.023c_1 - 0.037s_1,$ $^3F_2 = +0.009c_1 + 0.009s_1$	0.73	1.9
	total			38.2	100
$B_s(2D_2')$	$B_s(1^3P_2)\gamma$	532.11	$\langle 1^3P_2 r 2^3D_2 \rangle = 0.44889$	0.00001	~ 0
	$B_s(2^3P_2)\gamma$	185.16	$\langle 2^3P_2 r 2^3D_2 \rangle = 6.5948$	0.0001	0.0003
	KB^*		$^3D_2 = -0.059c_1 - 0.048s_1,$ $^3F_2 = +0.057c_1 - 0.070s_1$	26.65	79.31
	ηB_s^*		$^3D_2 = -0.037c_1 - 0.023s_1,$ $^3F_2 = +0.010c_1 - 0.009s_1$	6.98	20.77
	total			33.6	100

TABLE XXI: Our assignments for the observed B and B_s states are based on their masses, J^P and decay widths. Experimental masses and J^P for the states are taken from PDG [35] and theoretical masses are calculated by using a potential model discussed in Sec.(II). In the 4th column, there are two experimental masses, first for $B^0(d\bar{b})$ and second for $B^+(u\bar{b})$.

State	J^P	Our assignment	Experimental mass (MeV)	Theoretical mass (MeV)
$B_1(5721)$	1^+	$B(1P_1)$	5726.0 ± 1.3 $5725.9^{+2.5}_{-2.7}$	5755.12
$B_2^*(5747)$	2^+	$B(1^3P_2)$	5739.5 ± 0.7 5737.2 ± 0.7	5768.95
$B_J(5970)$...	$B(1^3D_1)$	5971 ± 5 5964 ± 5	6022.39
$B_{s1}(5830)$	1^+	$B_s(1P_1)$	5828.63 ± 0.27	5800.95
$B_{s2}^*(5840)$	2^+	$B_s(1^3P_2)$	5839.84 ± 0.18	5821.53

VI. CONCLUSIONS

We have computed the spectrum of B and B_s mesons up to $2F$ states with a nonrelativistic quark model that incorporates “scalar” confinement and one gluon exchange spin-dependent interactions. The eigenfunctions were then used to obtain E1 and M1 radiative transitions using the nonrelativistic reduction of the transition amplitude in impulse approximation. Strong decay amplitudes have also been obtained using the 3P_0 pair creation model and fitted SHO wavefunctions.

A comparison to four recently found B and B_s mesons with known J^P reveals good agreement with their natural candidate states in terms of mass and measured strong decay widths. The $B_J(5840)$ and $B_J(5970)$ are tougher to identify because their spin-parity has not been measured. However, we find that the lighter signal matches well with expectations for a 2^1S_0 state, while the $B_J(5970)$ is most naturally identified with the 1^3D_1 quark model state.

At present, excited states of the B and B_s mesons beyond P-wave have not been identified. We nevertheless expect that the LHCb collaboration will play a very important role in the study of excited states of the B and B_s meson families. The spectrum, radiative transitions, and strong decay widths presented here should prove helpful in the search for,

and interpretation of, these states.

VII. ACKNOWLEDGEMENT

B. Masud and F. Akram acknowledge the financial support of Punjab University.

-
- [1] V. M. Abazov *et al.* (DO Collaboration), Phys. Rev. Lett. 99, 1720001 (2007).
 - [2] R. Aaij *et al.* (LHCb Collaboration), Phys. Rev. Lett. 110, 151803 (2013).
 - [3] T. Aaltonen *et al.* (CDF Collaboration), Phys. Rev. D 90, 012013 (2014).
 - [4] R. Aaij *et al.* (LHCb Collaboration), JHEP **1504**, 024 (2015).
 - [5] Nosheen Akbar, Bilal Masud, Saba Noor, Eur. Phys. J. A (2011) 47: 124.
 - [6] M. Atif Sultan, Nosheen Akbar, Bilal Masud, and Faisal Akram, Phys. Rev. D 90, 054001 (2014).
 - [7] K. J. Juge, J. Kuti, and C. J. Morningstar, Phys. Rev. Lett., 82, 4400 (1999).
 - [8] Eric Braaten, Christian Langmack, and D. Hudson Smith, Phys. Rev. D 90, 014044 (2014).
 - [9] W. Lucha, H. Ruprecht, and F. Schoberl, Phys. Rev. D 46, 1088 (1992).
 - [10] J. F. Gunion, and L. F. Li., Phys. Rev. D 12, 3583 (1975).
 - [11] Nosheen Akbar, M. Atif Sultan, Bilal Masud, and Faisal Akram, Phys. Rev. D 95, 074018 (2017).
 - [12] K.A. Olive *et al.* (Particle Data Group), Chin. Phys. C, 86, 090001 (2014).
 - [13] D. Ebert, R.N. Faustov, V.O. Galkin, Eur. Phys. J. C 66 (2010).
 - [14] L. Micu, Nucl. Phys. B10, 521 (1969).
 - [15] A. Le Yaouanc, L. Oliver, O. Pene and J. Raynai, Phys. Rev. D8, 2223 (1973).
 - [16] A. Le Yaouanc, L. Oliver, O. Pene and J. Raynai, Phys. Rev. D9, 1415 (1974).
 - [17] A. Le Yaouanc, L. Oliver, O. Pene and J. Raynai, Phys. Rev. D11, 1272 (1975).
 - [18] W. Roberts and B. Silvestre-Brac, Few-Body Syst. 11, 171 (1992).
 - [19] W. Roberts and B. Silvestre-Brac, Phys. Rev. D 57, 1694 (1998).
 - [20] S. Capstick, W. Roberts, Phys. Rev. D 47, 1994 (1992).
 - [21] S. Capstick, W. Roberts, Phys. Rev. D 49, 4570 (1994).
 - [22] W. Roberts, B. Silvestre-Brac, C. Gignoux, Phys. Rev. D 41, 182 (1990).

- [23] J. W. Alcock, M. J. Burfitt and W. N. Cottingham, Z. Phys. C 25, 161 (1984).
- [24] S. Kumano and V.R. Pandharipande, Phys. Rev. D 38, 146 (1988).
- [25] P. Geiger and E. Swanson, Phys. Rev. D50, 6855 (1994).
- [26] T. Barnes, F. E. Close, P. R. Page, and E. S. Swanson, Phys. Rev. D 55, 4157 (1997).
- [27] T. Barnes, N. Black, and P. R. Page, Phys. Rev. D 68, 054014 (2003).
- [28] T. Barnes, S. Godfrey, and E. S. Swanson, Phys. Rev. D 72, 054026 (2005).
- [29] F. E. Close, and E. S. Swanson, Phys. Rev. D 72, 094004 (2005).
- [30] Stephen Godfrey, Kenneth Moats and Eric S. Swanson, Phys. Rev. D 94, 054025 (2016).
- [31] Yu. S. Kalashnikova, Phys. Rev. D 72, 034010 (2005).
- [32] J. Ferretti, G. Galata, E. Santopinto, and A. Vassallo, Phys. Rev. C 86, 015204 (2012).
- [33] J. Ferretti, G. Galata, and E. Santopinto, Phys. Rev. C 88, 015207 (2013).
- [34] E. S. Ackleh, T. Barnes and E. S. Swanson, Phys. Rev. D 54 6811 (1996).
- [35] C. Patrignani *et al.* (Particle Data Group), Chin. Phys. C, 40, 100001 (2016).
- [36] Stephen Godfrey, Phys. Rev. D 70, 054017 (2004).
- [37] R. Aaij *et al.* (LHCb Collaboration), JHEP 1504, 024 (2015).

Appendix A: SHO β values and masses for light mesons

The light meson masses used to determine phase space and final state momenta are [12]: $\pi = 0.1372$, $\eta = 0.5478$, $\rho = 0.7752$, $\omega = 0.7826$, $K = 0.495$, $K^* = 0.894$, $\phi = 1.019$. The SHO β values used in this work are listed in Table XXII and XXIII which are obtained by using the technique described in Sec. III.

TABLE XXII: Fitted β values (GeV) for ub and sb .

$n \ ^{2S+1}L_J$	ub	sb
1^1S_0	0.405	0.429
1^3S_1	0.372	0.401
1^1P_1	0.295	0.318
1^3P_J	0.292	0.316
1^1D_2	0.264	0.286
1^3D_J	0.264	0.286
1^1F_3	0.248	0.269
1^3F_J	0.248	0.269
2^1S_0	0.323	0.346
2^3S_1	0.309	0.334
2^1P_1	0.271	0.293
2^3P_J	0.270	0.292
2^1D_2	0.251	0.272
2^3D_J	0.251	0.272
3^1S_0	0.280	0.301
3^3S_1	0.273	0.295
3^1P_1	0.252	0.272
3^3P_J	0.251	0.271
3^1D_2	0.239	0.258
3^3D_J	0.238	0.258
4^1S_0	0.256	0.276
4^3S_1	0.252	0.272

TABLE XXIII: Fitted β values (GeV) for light mesons.

$n \ ^{2S+1}L_J$	uu	us	ss
1^1S_0	0.489	0.506	0.337
1^3S_1	0.200	0.324	0.337